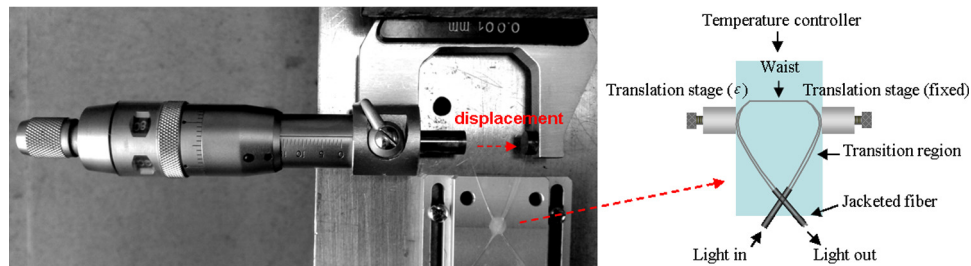


Temperature-Insensitive Microdisplacement Sensor Based on Locally Bent Microfiber Taper Modal Interferometer

Volume 4, Number 3, June 2012

Haimei Luo
Xinwan Li
Weiwen Zou
Xing Li
Zehua Hong
Jianping Chen



DOI: 10.1109/JPHOT.2012.2197606
1943-0655/\$31.00 ©2012 IEEE

Temperature-Insensitive Microdisplacement Sensor Based on Locally Bent Microfiber Taper Modal Interferometer

Haimei Luo,^{1,2} Xinwan Li,¹ Weiwen Zou,¹ Xing Li,¹
Zehua Hong,¹ and Jianping Chen¹

¹State Key Laboratory of Advanced Optical Communication Systems and Networks,
Department of Electronic Engineering, Shanghai Jiao Tong University, Shanghai 200240, China

²College of Physics and Communication Electronics, Jiangxi Normal University,
Nanchang 330022, China

DOI: 10.1109/JPHOT.2012.2197606
1943-0655/\$31.00 ©2012 IEEE

Manuscript received April 13, 2012; revised April 25, 2012; accepted April 25, 2012. Date of publication May 8, 2012; date of current version May 15, 2012. This work was supported in part by 973 program (ID2011CB301700), NSFC (ID61007052, 61107041, 61127016), STCSM Project (10DJ1400402), the International Cooperation Project from MOST (ID 2011FDA11780) and the “SMC Young Star” scientist Program of Shanghai Jiao Tong University. Corresponding authors: X. Li (e-mail: lixinwan@sjtu.edu.cn) and W. Zou (e-mail: wzou@sjtu.edu.cn).

Abstract: We report a temperature-insensitive microdisplacement sensor with a locally bent microfiber taper interferometer. The microfiber taper waist diameter can be optimized to minimize the spectral shift of the sensor owing to the environmental temperature change. With a $\sim 1.92 - \mu\text{m}$ -diameter microfiber taper, a bimodal fiber interferometer is proposed and experimentally fabricated. The transmission spectrum shows substantially small temperature dependence matching well with the theoretical estimation. The transmission spectrum is red-shifted in response to microdisplacement with a high sensitivity of $102 \text{ pm}/\mu\text{m}$ but without requirement for temperature compensation.

Index Terms: Microfiber taper, optical microdisplacement sensing, temperature-insensitive sensor, modal interferometer.

1. Introduction

In many industrial and scientific processes, microdisplacement sensing is required for precisely monitoring the movements in microelectromechanical systems (MEMS) and atomic force microscopy [1]–[3]. Due to the advantages of compact structure, low cost, easy fabrication, and high sensitivity, several optical fiber modal interferometer based microdisplacement sensors with a bent single-mode-fiber (SMF)-multimode fiber (MMF)-SMF [4], an embedded SMF-photonic-crystal-fiber (PCF)-SMF [5], and a SMF-polarization maintaining fiber (PMF)-SMF [6] structures were proposed recently. The bent SMF-MMF-SMF structure based sensor [4] provides superior sensitivity in comparison with the SMF-PCF-SMF [5] or SMF-PMF-SMF [6] based one due to the spectral interference. Optical fiber-taper-based modal interferometer can also be used for microdisplacement (or strain) sensing [7]–[9]. However, since a fiber taper is sensitive to both temperature and displacement (or strain) [7]–[10], it may cause great cross sensitivity and decrease the measurement accuracy when they are used for sensing displacement (or strain) in a variable temperature environment. Therefore, a concern associated with the use of fiber-taper-based modal interferometer sensors for displacement (or strain) measurement is removal of the thermal effect. Previously, we have reported the use of the locally bent microfiber taper structure [11] to construct a

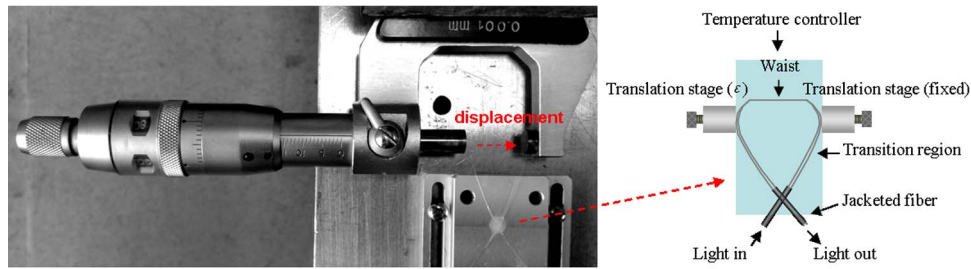


Fig. 1. Experimental setup and configuration of the sensor.

refractive index (RI) sensor that allowed for a higher sensitivity but a lower insertion loss than the S-tapered fiber interferometer based devices [9]. In this paper, we present the theoretical analysis and experimental study on the temperature dependence of a locally bent microfiber taper structure and its application to realize a temperature-insensitive microdisplacement sensor. The result shows that the temperature dependence of a locally bent microfiber taper strongly depends on the taper waist diameter and is possible to be minimized at a certain diameter range from $1.836 \mu\text{m}$ to $2.058 \mu\text{m}$. Using a $\sim 1.92 \mu\text{m}$ -diameter-waist microfiber taper, we demonstrate a temperature-insensitive microdisplacement sensor in the temperature range from 20°C to 80°C . The dependence of transmission spectrum on microdisplacement is theoretically and numerically analyzed. A high sensitivity of about $102 \text{ pm}/\mu\text{m}$ is experimentally observed, which is approximately 17 times higher than that of the bent SMF-MMF-SMF structure based displacement sensor [4] while its high temperature stability is comparable with respect to the one presented in [5] or [6].

2. Device Structure and Operating Principle

The experimental setup using a locally bent microfiber taper structure for microdisplacement sensing is shown in Fig. 1. The transition region of the microfiber taper was locally bent while the waist was pulled straightly. The X-shaped crossing section of the jacketed fiber was fixed by epoxy to a fiber holder. The locally bent microfiber taper structure was placed between two translation stages. One stage was fixed while the other was tuned to apply an incremental displacement to the device through the bent transmission region. The device is under temperature control for thermal stability test.

As described in [10], the light injected into the uniform taper waist from a locally bent transmission region excites high-order modes successively propagating in the waist. When these modes are coupled back into the fundamental mode in the output locally bent region, as a result of interference, the wavelength-dependent transmission spectrum is obtained.

When only one dominant high-order mode is considered, the phase difference φ between the fundamental mode (i.e., the HE_{11} mode) and the first excited high-order mode (i.e., the HE_{21} mode) is

$$\varphi = 2\pi\delta n_{\text{eff}}L/\lambda \quad (1)$$

where, L is the interferometer length, λ is the wavelength of light in vacuum and $\delta n_{\text{eff}} = n_1 - n_2$ with n_1 and n_2 being the effective indexes of the HE_{11} mode and HE_{21} mode, respectively. The attenuation peak wavelength λ_m of the locally bent microfiber taper modal interferometer can be expressed as [12]

$$\lambda_m = 2\delta n_{\text{eff}}L/(2m + 1) \quad (2)$$

where m is the interference order.

The temperature variation changes the phase difference due to the temperature dependence of δn_{eff} and L . Suppose that the thermo-optic coefficients are ζ_1 and ζ_2 for the two modes, respectively, thus $\Delta\delta n_{\text{eff}}$ and ΔL induced by the temperature variation ΔT can be given by $\Delta\delta n_{\text{eff}} = (\zeta_1 n_1 - \zeta_2 n_2)\Delta T$ and $\Delta L = \alpha L\Delta T$ where α is the thermal expansion coefficient of the silica fiber

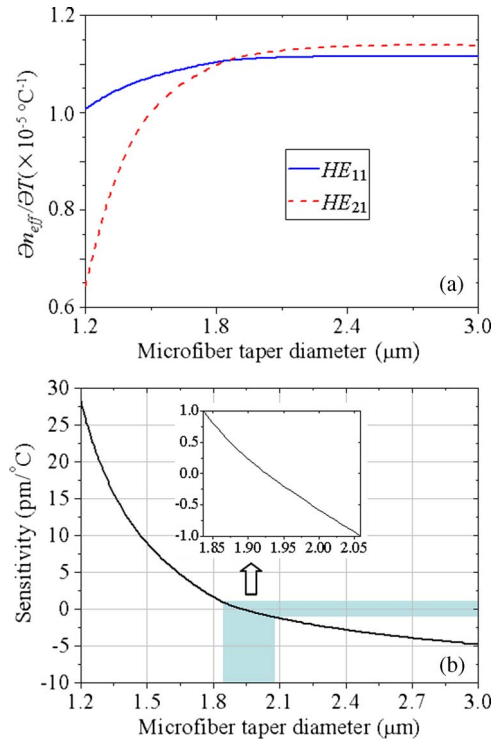


Fig. 2. (a) Calculated n_{eff}/T of the modes HE_{11} and HE_{21} for the wavelength $1.55 \mu\text{m}$ as a function of the microfiber taper waist diameter. (b) Calculated temperature sensitivity varying with microfiber taper waist diameter for temperature range of 20°C – 80°C ($\Delta T = 60^\circ\text{C}$).

being independent on optical modes. Therefore, the wavelength shift in response to temperature change can be expressed by

$$\Delta\lambda \approx [(\alpha + \zeta)\Delta T]\lambda \quad (3)$$

where, $\zeta = (\zeta_1 n_1 - \zeta_2 n_2)/\delta n_{\text{eff}}$, which corresponds to the thermal-induced variation of the effective index difference of the two modes.

We use the finite-element method (FEM) to numerically calculate the two propagating modes in order to analyze the taper geometrical effects on n_{eff} . Fig. 2(a) shows the calculated $\partial n_{\text{eff}}/\partial T$ of the modes HE_{11} and HE_{21} for the wavelength of $1.55 \mu\text{m}$ as a function of the microfiber taper waist diameter. The constants of the thermal coefficient of the RI and thermal expansion coefficient in silica glass are $\partial n_{\text{eff}}/\partial T = 1.1 \times 10^{-5}/^\circ\text{C}$ and $\alpha = 5.5 \times 10^{-7}/^\circ\text{C}$ [13]. From Fig. 2(a), it can be seen that ζ being a function of the fiber profile can be either positive or negative depending on the fiber diameter, which is in contrary to the thermal change of the RI alone. At a particular diameter, the negative ζ can compensate the thermal expansion effect, i.e., $-\zeta = \alpha$. In consequence, the wavelength shift can be zero. Fig. 2(b) shows the calculated temperature-dependence sensitivity varying with microfiber taper waist diameter for temperature range of 20°C – 80°C ($\Delta T = 60^\circ\text{C}$). It is noted that the wavelength shift becomes less than $1 \text{ pm}/^\circ\text{C}$ in the diameter range from $1.836 \mu\text{m}$ to $2.058 \mu\text{m}$ marked in Fig. 2(b).

When a displacement of ε is incrementally applied on the sensor, the bending radius of the transition region of the microfiber taper is increased from R_0 to R . As a result, the effective interference length is decreased by ε . According to the fiber geometry shown in Fig. 3, the change of the bend radius (ΔR) can be expressed by

$$\Delta R = R - R_0 = \frac{R_0 \varepsilon + \varepsilon^2}{R_0 - \varepsilon}. \quad (4)$$

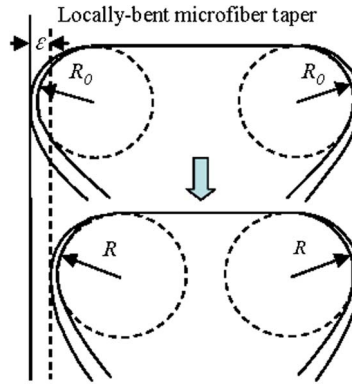


Fig. 3. Schematic of the bent ultrathin fiber taper structure for the proposed microdisplacement sensor.

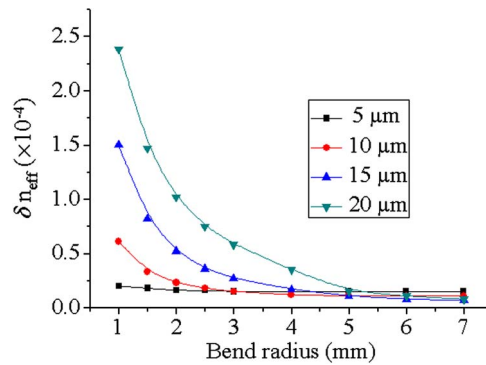


Fig. 4. Calculated dependence of δn_{eff} on the initial bend radius (R_0) and fiber diameter (d) of the bent transition region at the wavelength of $1.55 \mu\text{m}$.

The above equation shows that the change of the bend radius (ΔR) is approximately a linear function of the applied displacement, i.e., $\Delta R \approx \varepsilon$ since $\varepsilon \ll R_0$.

Due to the change of the bending radius (ΔR), the condition for the fundamental mode coupling with the high-order mode suffers variation, leading to the variation of the effective index difference of the two modes. The wavelength shift $\Delta\lambda$ induced by the change of the bend radius can be given by

$$\frac{\Delta\lambda}{\lambda} = \left(\frac{1}{\delta n_{eff}} \frac{d\delta n_{eff}}{dR} + \frac{1}{L} \frac{dL}{dR} \right) \Delta R. \quad (5)$$

To determine the effects of displacement on δn_{eff} of the fundamental mode and the high-order mode, we numerically calculated the dependence of δn_{eff} on the initial bend radius (R_0) and fiber diameter of the bent transition region at the wavelength of $1.55 \mu\text{m}$. The simulated results are shown in Fig. 4. In the calculation, the equivalent RI distribution for the bent microfiber taper section is $n = n_0[1 + (1 + \chi)x/R]$ [14], where n_0 is the RI profile when the fiber is straight, R is the bend radius, x is a transverse co-ordinate along a line joining the center of curvature and the center of the fiber, and $\chi = -0.22$ denotes the elasto-optic effect for silica [14]. From the results, one can see that the bent transition region of the fiber taper with higher diameter d or smaller initial bend radius R_0 exhibits higher sensitivity. The larger the bend radius R , the smaller the effective index difference δn_{eff} .

3. Experimental Investigation

Experimental investigations were carried out for the proposed microdisplacement sensor. The microfiber taper was drawn from a standard Corning SMF-28 fiber with the flame-heated taper-drawing technique [15], [16]. The SMF has the core (cladding) diameter of $8.2 \mu\text{m}$ ($125 \mu\text{m}$) and the

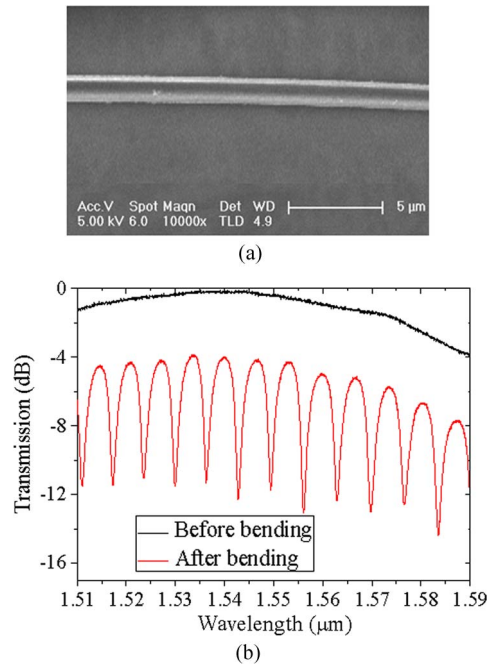


Fig. 5. (a) SEM image of the fiber taper waist with diameter of $\sim 1.92 \mu\text{m}$. (b) Transmission spectrum of the optical fiber before and after bending.

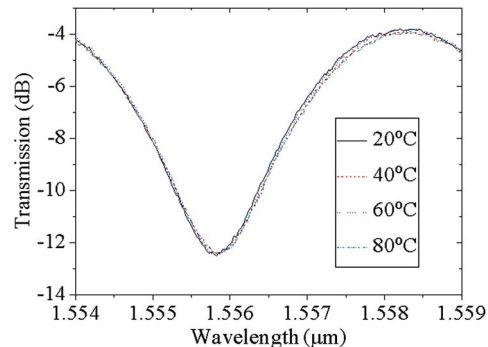


Fig. 6. Measured transmission spectra under different temperatures.

RI of the core (cladding) of 1.454 (1.4505) at the wavelength of $1.55 \mu\text{m}$. The taper waist is about 8 mm in length and $\sim 1.92 \mu\text{m}$ in diameter. Each side of the transition region is about 17 mm long. Fig. 5(a) shows the SEM image of the taper waist. The bending occurs symmetrically in the two transition regions with bending radius $R_0 = \sim 3 \text{ mm}$, while the waist remains straight. The transmission spectrum of the interferometer ranging from $1.51 \mu\text{m}$ to $1.59 \mu\text{m}$ is measured using a broadband light source and an optical spectrum analyzer (OSA) (Yokogawa AQ6370B). As shown in Fig. 5(b), the transmission spectrum before bending corresponds to the transmission loss of the fiber taper itself, which means the tapering process is adiabatic and there is no power transfer between different modes [17]. In comparison, after bending, the HE_{21} mode is mainly excited and an interference transmission pattern between the fundamental mode (HE_{11} mode) and the excited high-order mode (HE_{21} mode) is obtained [10]. The total insertion loss is around 4.2 dB due to bending loss at both bent transition regions. The extinction ratio of the pattern is about 10 dB.

First, we measured the temperature independence of the interferometer by placing it inside a temperature-controlled chamber. The attenuation peak at the wavelength of $1.5559 \mu\text{m}$ red-shifts

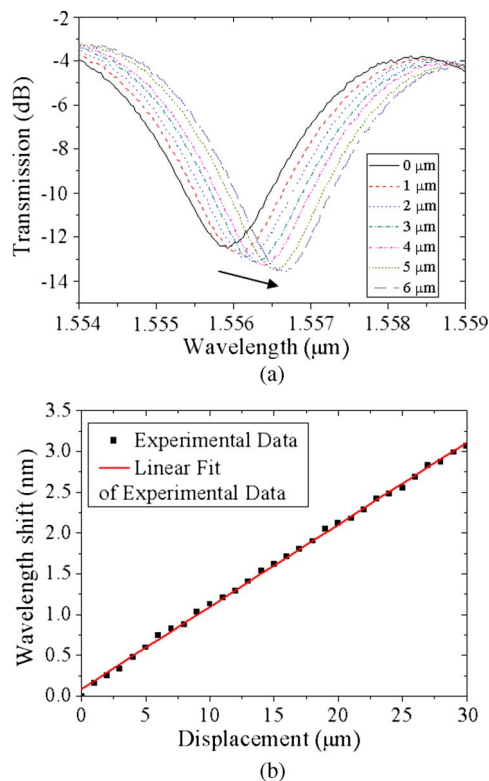


Fig. 7. (a) Measured spectra for various displacements. (b) The wavelength shift of the transmission dips versus the displacement of the locally bent fiber taper structure.

slightly toward longer wavelength when temperature changes from 20 °C to 80 °C, as shown in Fig. 6. The temperature coefficient of the transmission dip is estimated to be ~ 0.45 pm/°C, which agrees well with the theoretical results. So temperature influence on the interferometer can be neglected when operated in normal environmental condition.

Second, different displacement was applied to the device through the tunable translation stage with a motion accuracy of 1 μm (see Fig. 3). Fig. 7(a) demonstrates the measured transmission spectra of the same attenuation peak under different displacement ε . It is noted that an obvious wavelength red-shift of the transmission spectrum (dip) can be observed even when the displacement ε is only 1 μm . The displacement not only shortens the interference length L but also increases the bending radius R , which results in a decrease in the δn_{eff} . According to (2), the attenuation peak wavelength shifts toward longer wavelength with displacement increasing. Fig. 7(b) summarizes the wavelength shift of the spectral dip as a function of the displacement ε . The black squares are the measured results and the red solid line represents a least-squares linear fitting. In the displacement range of 0–30 μm , the wavelength shift was linearly proportional to the displacement. The displacement sensing sensitivity is deduced to be 102 pm/ μm .

4. Conclusion

In summary, we have proposed a fiber microdisplacement sensor by using a locally bent microfiber taper modal interferometer as the sensing element. Theoretical investigation shows that the temperature dependence of a locally bent microfiber taper strongly relates to the microfiber taper waist diameter and it is possible to minimize the temperature dependence at a certain diameter range from 1.836 μm to 2.058 μm . A fabricated locally bent microfiber taper with diameter of ~ 1.92 μm shows an ultralow temperature sensitivity of ~ 0.45 pm/°C in the temperature range from 20 °C to 80 °C. The dependence of the spectrum shift in response to displacement has been

derived and its sensitivity of 102 pm/ μm has been experimentally characterized. This performance can be improved, for example, using the locally bent microfiber taper structure with a smaller initial bend radius. Compared with other fiber modal interferometer based microdisplacement sensors [2]–[9], the proposed one is insensitive to temperature eliminating the requirement for temperature compensation, and provides higher sensitivity due to the spectral measurement.

References

- [1] H. Baltes, O. Brand, G. K. Fedder, C. Hierold, J. G. Korvink, and O. Tabata, *Book Series Advanced Micro & Nanosystem*. Weinheim, Germany: Wiley-VCH, 2004–2006.
- [2] O. Levy, B. Z. Steinberg, M. Nathan, and A. Boag, “Ultrasensitive displacement sensing using photonic crystal waveguides,” *Appl. Phys. Lett.*, vol. 86, no. 10, p. 104 102, Mar. 2005.
- [3] Z. Xu, L. Cao, C. Gu, Q. He, and G. Jin, “Micro displacement sensor based on line-defect resonant cavity in photonic crystal,” *Opt. Exp.*, vol. 14, no. 1, pp. 298–305, Jan. 2006.
- [4] Q. Wu, A. M. Hatta, P. Wang, Y. Semenova, and G. Farrell, “Use of a bent single SMS fiber structure for simultaneous measurement of displacement and temperature sensing,” *IEEE Photon. Technol. Lett.*, vol. 23, no. 2, pp. 130–132, Jan. 2011.
- [5] B. Dong and J. Hao, “Temperature-insensitive and intensity-modulated embedded photonic-crystal-fiber modal-interferometer-based microdisplacement sensor,” *J. Opt. Soc. Amer. B, Opt. Phys.*, vol. 28, no. 10, pp. 2332–2336, Oct. 2011.
- [6] C. Zhong, C. Shen, Y. You, J. Chu, X. Zou, X. Dong, Y. Jin, and J. Wang, “Temperature-insensitive optical fiber two-dimensional micrometric displacement sensor based on an in-line Mach–Zehnder interferometer,” *J. Opt. Soc. Am. B*, vol. 29, no. 5, pp. 1136–1140, May 2012.
- [7] K. Q. Kieu and M. Mansuripur, “Biconical fiber taper sensors,” *IEEE Photon. Technol. Lett.*, vol. 18, no. 21, pp. 2239–2241, Nov. 2006.
- [8] Z. Tian and S. S.-H. Yam, “In-line abrupt taper optical fiber Mach–Zehnder interferometric strain sensor,” *IEEE Photon. Technol. Lett.*, vol. 21, no. 3, pp. 161–163, Feb. 2009.
- [9] R. Yang, Y. S. Yu, Y. Xue, C. Chen, Q. D. Chen, and H. B. Sun, “Single S-tapered fiber Mach–Zehnder interferometers,” *Opt. Lett.*, vol. 36, no. 23, pp. 4482–4484, Dec. 2011.
- [10] P. Lu, L. Men, K. Sooley, and Q. Chen, “Tapered fiber Mach–Zehnder interferometer for simultaneous measurement of refractive index and temperature,” *Appl. Phys. Lett.*, vol. 94, no. 13, p. 131 110, Apr. 2009.
- [11] H. M. Luo, X. W. Li, W. W. Zou, W. N. Jiang, and J. P. Chen, “Modal interferometer based on a C-shaped ultrathin fiber taper for high-sensitivity refractive index measurement,” *Appl. Phys. Exp.*, vol. 5, no. 1, p. 012502, Jan. 2012.
- [12] T. Allsop, R. Reeves, D. J. Webb, I. Bennion, and R. Neal, “A high sensitivity refractometer based upon a long period grating Mach–Zehnder interferometer,” *Rev. Sci. Instrum.*, vol. 73, no. 4, pp. 1702–1705, Jan. 2012.
- [13] Y. Chen, F. Xu, and Y. Q. Lu, “Teflon-coated microfiber resonator with weak temperature dependence,” *Opt. Exp.*, vol. 19, no. 23, pp. 22 923–22 928, Nov. 2011.
- [14] H. F. Taylor, “Bending effects in optical fibers,” *J. Lightw. Technol.*, vol. 2, no. 5, pp. 617–628, Oct. 1984.
- [15] L. M. Tong, R. P. Gattass, J. B. Ashcom, S. L. He, J. Y. Lou, M. Y. Shen, and I. Mazur, “Subwavelength-diameter silica wires for low-loss optical wave guiding,” *Nature*, vol. 426, no. 6968, pp. 816–819, Dec. 2003.
- [16] Z. H. Hong, X. W. Li, L. Zhou, X. W. Shen, J. G. Shen, S. G. Li, and J. P. Chen, “Coupling characteristics between two conical micro/nano fibers: Simulation and experiment,” *Opt. Exp.*, vol. 19, no. 5, pp. 3854–3861, Feb. 2011.
- [17] J. D. Love, W. M. Henry, W. J. Stewart, R. J. Black, S. Lacroix, and F. Gonthier, “Tapered single-mode fibers and devices. Part 1: Adiabaticity criteria,” *Proc. Inst. Elect. Eng. J—Optoelectron.*, vol. 138, no. 5, pp. 343–354, Oct. 1991.